

Secure Aggregation Meets Sparsification in Decentralized Learning

Sayan Biswas
EPFL

Anne-Marie Kermarrec
EPFL

Rafael Pires
EPFL

Rishi Sharma
EPFL

Milos Vujasinovic
EPFL

Abstract

Decentralized learning (DL) faces increased vulnerability to privacy breaches due to sophisticated attacks on machine learning (ML) models. Secure aggregation is a computationally efficient cryptographic technique that enables multiple parties to compute an aggregate of their private data while keeping their individual inputs concealed from each other and from any central aggregator. To enhance communication efficiency in DL, sparsification techniques are used, selectively sharing only the most crucial parameters or gradients in a model, thereby maintaining efficiency without notably compromising accuracy. However, applying secure aggregation to sparsified models in DL is challenging due to the transmission of disjoint parameter sets by distinct nodes, which can prevent masks from canceling out effectively. This paper introduces CESAR, a novel secure aggregation protocol for DL designed to be compatible with existing sparsification mechanisms. CESAR provably defends against honest-but-curious adversaries and can be formally adapted to counteract collusion between them. We provide a foundational understanding of the interaction between the sparsification carried out by the nodes and the proportion of the parameters shared under CESAR in both colluding and non-colluding environments, offering analytical insight into the working and applicability of the protocol. Experiments on a network with 48 nodes in a 3-regular topology show that with random subsampling, CESAR is always within 0.5% accuracy of decentralized parallel stochastic gradient descent (D-PSGD), while adding only 11% of data overhead. Moreover, it surpasses the accuracy on TopK by up to 0.3% on independent and identically distributed (IID) data.

1 Introduction

Large and high-quality datasets play a major role in unlocking the full potential of machine learning (ML) models [20,35,52]. Collaborative learning, by pooling datasets from multiple sources, enables the creation of more robust and diverse ML

models. However, the direct sharing of data for ML training poses significant privacy and security challenges, especially in domains where data is sensitive or regulated, such as under the general data protection regulation (GDPR) [13] and the health insurance portability and accountability act (HIPAA) [43].

To address these challenges, Federated learning (FL) [30] and Decentralized learning (DL) [25] have been developed to enable the training of ML models without direct data sharing. In these paradigms, data remains distributed across nodes (user devices or servers), and learning is achieved through the exchange of model parameters or updates, rather than raw data. This approach enhances privacy, as data does not leave its original location, and scales efficiently to large numbers of participants.

While FL has been utilized in various domains including text prediction [6,34,47] and healthcare [19,21,28], DL offers a distinct advantage in scenarios where a centralized coordinating server is infeasible or undesirable. DL, by decentralizing the learning process, further empowers data privacy and local control, making it particularly attractive for applications that require distributed decision-making and autonomy over data.

Despite these advantages, DL faces its own set of significant challenges, particularly in terms of communication efficiency and privacy preservation. The transmission of model parameters, especially in deep learning networks, can lead to substantial communication overhead. To mitigate this, sparsification techniques are employed. The TOPK [3] method, for instance, focuses on transmitting only the top k parameters with the highest gradients, while random subsampling [22,42] involves randomly selecting a subset of parameters for transmission. Additionally, techniques like Jwins [10] use wavelet transforms to rank the parameters without significant loss of information. These approaches aim to reduce the volume of data transmitted, concentrating on the most impactful parameters or gradients to preserve the model’s accuracy.

However, the application of secure aggregation protocols to sparsified models in DL introduces unique challenges. These protocols employ coordinated random masks added to the pa-

rameters by each participant. When aggregated, these masks are designed to cancel out, thereby revealing only the aggregate result and not the individual data contributions, effectively preserving the privacy of each participant. Nevertheless, when sparsification is employed, the transmission of disjoint sets of parameters by different nodes can disrupt the effective cancellation of these cryptographic masks in secure aggregation. This disruption leads to inaccurate results due to residual noise not being fully negated.

Moreover, another critical aspect in the interplay of sparsification and secure aggregation in DL is the alignment of parameter indices. Sparsification techniques such as TopK and random subsampling, by their nature, select different sets of parameters across nodes. When these nodes engage in secure aggregation, a crucial requirement is the matching of indices to ensure that masks cancel out properly. However, this necessity often leads to a further reduction in the number of parameters being aggregated, as any non-matching indices must be discarded to avoid non-canceled noise. This additional layer of parameter reduction can potentially impact the convergence of the model, as important parameters might be excluded from the aggregation process. Understanding and addressing this intersection challenge is key to optimizing the balance between privacy preservation, efficient communication and model accuracy in DL.

To address these challenges, this paper introduces Communication-efficient secure aggregation (CESAR), a novel protocol designed for decentralized learning. CESAR is uniquely engineered to be compatible with various forms of sparsification. The protocol is robust against honest-but-curious adversaries and can be adapted to resist collusion attacks by introducing a trade-off in communication efficiency. Our comprehensive experiments conducted on several k -regular graph topologies demonstrate that CESAR, when employed with random subsampling, matches the performance of decentralized parallel stochastic gradient descent (D-PSGD) with only a modest increase in data overhead. Moreover, CESAR shows superior accuracy compared to TOPK sparsification methods, affirming its effectiveness in striking a balance between communication efficiency, privacy preservation, and model accuracy in decentralized learning environments.

In this paper, we make the following contributions:

- We introduce CESAR, the first protocol for secure aggregation in decentralized learning using sparsification techniques.
- We formally show that our protocol is secure against honest-but-curious users and provide a theoretical analysis that enables CESAR to be provably resilient against colluding nodes.
- We theoretically derive the anticipated quantity of shared parameters between nodes within CESAR in the presence of colluding adversaries in the network. This allows us to parameterize the utility of CESAR and offers analytical insights into the workings and applicability of the protocol.
- We evaluated the performance and communication costs of our protocol across three distinct datasets within two different application domains. Our results demonstrate that CESAR can replace D-PSGD without the need for altering hyperparameters, while still preserving comparable levels of performance. Furthermore, an extensive analysis on CIFAR-10 showed CESAR can surpass the accuracy of D-PSGD, while sharing as little as 7% additional data using random subsampling, and 12% using TOPK sparsification.

The remaining of this paper is organized as follows. Section 2 briefly introduces the concept of DL, Sparsification and Secure Aggregation. CESAR is described in Section 3, along with the corresponding analysis. We empirically evaluate CESAR in Section 4 under several aspects. Related work is surveyed in Section 5 before a brief discussion (Section 6) and the conclusion in Section 7.

2 Preliminaries

2.1 Decentralized Learning

Decentralized learning is a form of machine learning involving a set of nodes \mathcal{N} organized in a network topology G . Each node, labeled as $N_i \in \mathcal{N}$, has its local dataset D_i characterized by its distribution ϕ_i . During training, these local datasets remain private and are not shared among nodes. If local label distributions are homogeneous across nodes, we call these datasets independent and identically distributed (IID), and non-IID otherwise.

The collective objective of the training is to find a set of optimal parameters θ^* that minimizes a loss function \mathcal{L} across the aggregated dataset of all nodes, represented as $D = \bigcup_{N_j \in \mathcal{N}} D_j$:

$$\theta^* = \arg \min_{\theta} \mathcal{L}(D; \theta)$$

The training happens over multiple rounds, each comprised of three steps: training, sharing, and aggregation. Initially, each node performs one or several iterations of an optimization algorithm, typically stochastic gradient descent (SGD), on mini-batches of their local dataset. After this, they share their updated parameters either to all neighbors in the network topology, as in D-PSGD [26], or to a selected subset of neighbors, as in random model walk (RMW) [31]. Finally, upon receiving parameters from their neighbors, each node computes an average of these parameters together with its own model. This newly computed averaged parameter set then becomes the starting point for the next round of training. The process is iterated until convergence.

2.2 Sparsification

Machine learning models are often large and become even more so, which incurs significant costs when transferring them over a network. Sparsification is a technique for lossy model compression. This technique assumes that even a subset of the parameters of a model carries important information about the model. Therefore, it involves transmitting a selected subset of indices, rather than the entire model.

Two popular sparsification approaches are random subsampling [22, 42] and TopK [3]. Both take as input the percentage of indices to be selected, denoted as α , and a model of size k . Random subsampling samples each index with a probability of α , ultimately expecting to select αk indices. The indices selected in TopK, on the other hand, depend on their magnitude: they are first sorted by weight and the top αk with highest values are chosen. While TopK preserves crucial features by prioritizing significant parameters, it risks overfitting as some parameters are never shared. Random subsampling, in turn, does not induce overfitting but may lead to loss of important information and hence lead to lower accuracy.

2.3 Secure Aggregation

Secure aggregation [4] is a form of multiparty computation, *i.e.*, a technique allowing multiple parties to jointly compute a function over their inputs while keeping those inputs private. It is performed by a set of $p \geq 3$ nodes $\mathcal{N} = \{N_1, N_2, \dots, N_p\}$. Every node N_i has a private value x_i that it wants to keep private and yet use it to calculate the value of a function $f(x_1, x_2, \dots, x_p) = \sum_{i=1}^p x_i =: \hat{x}$ together with other nodes from \mathcal{N} . At the end of the protocol, every value x_i must remain private, while the aggregated value \hat{x} is public.

Pairwise masking [1, 4] is a prominent way of performing secure aggregation. This approach assumes an imposed ordering of nodes: $N_1 < N_2 < \dots < N_p$. Under this assumption every pair of nodes N_i, N_j (where $N_i < N_j$) collaboratively generates a private random mask $M_{i,j}$. The masking process involves N_i adding $M_{i,j}$ to its value, and N_j subtracting the same mask from its value. The masks applied in this fashion sum up to 0, guaranteeing that the sum of masked values is equal to the sum of original values. Applying this technique across all node pairs, each node N_i computes a masked value $x'_i = x_i - \sum_{j=1}^{i-1} M_{j,i} + \sum_{j=i+1}^p M_{i,j}$. The resulting masked value, x'_i , can be safely shared publicly, as it reveals no information about the original value x_i .

3 CESAR: Secure aggregation for sparsified decentralized learning

3.1 System model

We consider a set of n nodes, denoted as $\mathcal{N} = \{N_1, \dots, N_n\}$, interconnected in a communication graph $G(\mathcal{N}, E)$. We con-

sider all communication channels to be bidirectional (*e.g.*, TCP connections over the Internet) and assume there exists an underlying mechanism used for generating another graph called *aggregation graph*. This aggregation graph is a spanning subgraph of the original communication graph (*i.e.*, an overlay network). For clarity, all subsequent mentions of a graph in this paper will specifically refer to the aggregation graph.

The protocol requires each node to communicate not only with its immediate neighbors but also with the neighbors of these neighbors. Consequently, we assume that each node must possess knowledge of both these types of nodes within the graph. We denote immediate neighbors of $N \in \mathcal{N}$ as $\text{View}(N) = \{M : M \in \mathcal{N} \wedge \{N, M\} \in E\}$ and second degree neighbors as $\text{View}_2(N) = (\cup_{M \in \text{View}(N)} \text{View}(M)) \setminus \{N\}$. For $N_\ell, N_i \in \mathcal{N}$, if $\{N_\ell, N_i\} \in E$, let $\text{Comm}(N_\ell, N_i) = \text{View}(N_\ell) \setminus \{N_i\}$ denote the set of all nodes in the network that N_i communicates with to find out the intersection of the sampled parameters, agree upon the mask to be applied to them, and, in turn, share these masked parameters to N_ℓ . In this context, we refer to N_ℓ as the *receiving node* of N_i 's masked model parameters. We assume that each communication channel is secure and encrypted, and subsequently that it cannot be eavesdropped. However, there are no definitive guarantees of direct communication channels for nodes that are two hops away (distance 2) in the aggregation graph. Therefore, when second degree neighbors attempt to communicate and lack a direct channel in the communication graph, the common neighbor must relay their messages. This process effectively doubles the total number of messages sent in such scenarios. Nevertheless, in real-life systems, the communication graph is almost always near-fully connected, which typically circumvents this issue. For simplicity, the rest of this paper assumes that the communication graph is fully connected.

All nodes train models with a shared architecture, each having d parameters and being characterized by identical numbers of layers and corresponding layers of same shape. Parameters are enumerated using indices, or parameter position used interchangeably, $I = \{1, \dots, d\}$. Parameters held by N_i are denoted as $v_i \in \mathbb{R}^d$ where $v_i^{(p)}$ denotes the value of the parameter at index p and node N_i . The set of indices selected for sharing by N_i in DL is denoted as $I_i \subseteq I$

3.2 Threat model

In the scope of this work, we primarily focus on the threat posed by honest-but-curious adversaries. Accordingly, all nodes in our threat model adhere to the protocol and do not collude with each other. However, they attempt to infer as much information as possible from the data accessible to them through the protocol.

Section 3.4.2 steps out of this threat model looking into possible presence of colluding adversaries in the system and proposes ways to adjust the protocol in order to combat them.

3.3 Algorithm

In this subsection we introduce the protocol, CESAR. The pseudo-code of the protocol is shown in Algorithm 1 and the overview of execution in Figure 1. The algorithm is broken into subcomponents for readability and ease of understanding.

Algorithm 1: CESAR running in parallel on every Node N_i

Input: Accepts list of indices selected in sparsification $I_i \subseteq I = \{1, 2, 3, \dots, d\}$, all current local parameters of $v_i \in \mathbb{R}^d$, and aggregation graph $G(\mathcal{N}, E)$ in which aggregation takes place

Output: The aggregated model $v'_i \in \mathbb{R}^d$ of the neighborhood of the node

```

1  $M'_i, I_{i\cap} \leftarrow \text{prestep}(N_i, I_i)$ 
2  $\text{send\_masked\_models}(N_i, v_i, M'_i, I_{i\cap})$ 
3 return  $\text{aggregate\_received\_models}(N_i, v_i)$ 

```

Algorithm 2: CESAR-prestep

```

1 Function  $\text{prestep}(N_i, I_i)$ 
2   for  $N_j \in \text{View}_2(N_i)$  do
3     Generate pseudo-random number  $\text{seed}_{ij}$ 
4     Send  $(I_i, \text{seed}_{ij})$  to node  $N_j$ 
5   for  $N_j \in \text{View}_2(N_i)$  do
6      $(I_j, \text{seed}_{ji}) \leftarrow \text{Receive from node } N_j$ 
7      $I_{i\cap j} \leftarrow I_i \cap I_j$ 
8      $M_{ij} \leftarrow \text{Random mask over } I_{i\cap j} \text{ with seed } \text{seed}_{ij}$ 
9      $M_{ji} \leftarrow \text{Random mask over } I_{i\cap j} \text{ with seed } \text{seed}_{ji}$ 
10     $M'_{ij} \leftarrow M_{ij} - M_{ji}$ 
11   $M'_i \leftarrow \cup_{N_j \in \mathcal{N}} M'_{ij}$ 
12   $I_{i\cap} \leftarrow \cup_{N_j \in \mathcal{N}} I_{i\cap j}$ 
13  return  $M'_i, I_{i\cap}$ 

```

The inputs of the protocol are current model parameters, the set of indices selected by the sparsification algorithm and the network graph. This protocol builds upon D-PSGD using pairwise additive masking to implement secure aggregation. Pairwise masking is the standard way of doing secure aggregation within FL [4].

In D-PSGD, models are broadcast to all adjacent nodes. A notable challenge emerges when considering a node, let us call it N_1 , transmitting its model to neighboring nodes $N_{n_1}, N_{n_2}, \dots, N_{n_k}$. Each of these neighbors, N_{n_i} , also receives models from their respective neighbors. In an arbitrary network graph, it is not guaranteed that the nodes $N_{n_1}, N_{n_2}, \dots, N_{n_k}$ share any common neighbors besides N_1 . Consequently, if N_1 wishes to send the same masked model to all its neighbors, it would require at least one unique counter-

Algorithm 3: CESAR-masking the model and sending it to the neighbors

```

1 Function  $\text{send\_masked\_models}(N_i, v_i, M'_i, I_{i\cap})$ 
2   for  $N_k \in \text{View}(N_i)$  do
3      $v_{k\leftarrow i} \leftarrow v_i$ 
4      $C \leftarrow \text{Zero vector of size } d$ 
5     for  $N_j \in \text{View}(N_k) \setminus \{N_i\}$  do
6        $v_{k\leftarrow i}[I_{i\cap j}] \leftarrow v_{k\leftarrow i}[I_{i\cap j}] + M'_{ij}$ 
7        $C[I_{i\cap j}] \leftarrow C[I_{i\cap j}] + 1$ 
8      $I'_{ik} \leftarrow p \in I : C[p] \geq 1$ 
9      $w_{k\leftarrow i} \leftarrow v_{k\leftarrow i}[I'_{ik}]$ 
10    Send  $(I'_{ik}, w_{k\leftarrow i})$  to node  $N_k$ 

```

Algorithm 4: CESAR-Aggregating received models

```

1 Function  $\text{aggregate\_received\_models}(N_i, v_i)$ 
2    $v'_i \leftarrow v_i$ 
3    $c \leftarrow 1$ 
4   for  $N_k \in \text{View}(N_i)$  do
5      $(I'_{ki}, w_{k\leftarrow i}) \leftarrow \text{Receive from node } N_k$ 
6      $v'_k \leftarrow v_i$ 
7      $v'_k[I'_{ki}] \leftarrow w_{k\leftarrow i}$ 
8      $v'_i \leftarrow v'_i + v'_k$ 
9      $c \leftarrow c + 1$ 
10   $v'_i \leftarrow \frac{v'_i}{c}$ 
11  return  $v'_i$ 

```

part node with exactly the same set of neighbors with whom it could agree on a pairwise mask. This condition is rarely met in most arbitrary graphs, leading us to adopt an alternative method.

In our protocol rather than sending a model masked with the same mask to all neighbors, a node transmits the same model, each time masked differently, to each neighbor. Specifically, a node coordinates with every neighbor of the intended recipient to establish a unique pairwise mask. When broadcasting a model, the node applies all the masks it has agreed upon with the neighbors of the recipient.

This approach is effective as long as the recipient has at least two neighbors and receives all the masked models from them. It ensures that every parameter received is masked at least once and that for each mask used to obfuscate a parameter, its counterpart (the opposite mask) is present among the other received masked models. Otherwise, if there is a node N_{single} with only a single neighbor, the given neighbor won't have another node to mask their parameters with and hence, following Algorithm 1, won't send any parameters to N_{single} making the given edge redundant.

Upon receiving all the masked models, the recipient aggregates them with their own model and computes the average. This process results in a new model that aligns with the result

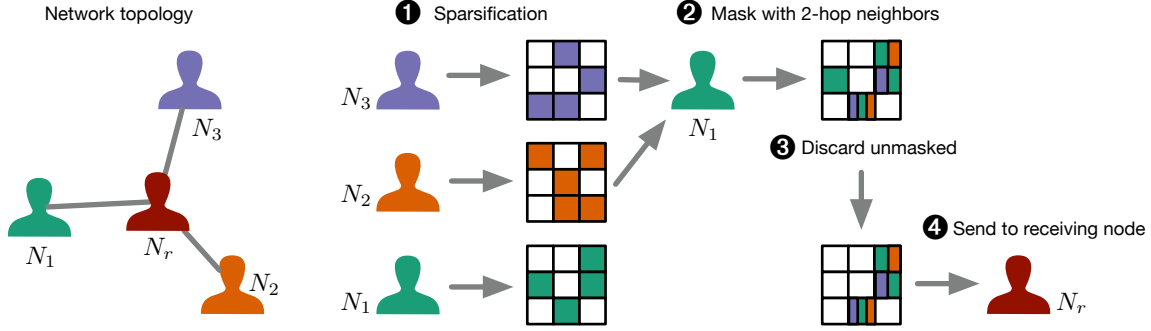


Figure 1: Overview of CESAR model masking on N_1 . (1) Nodes N_1 , N_2 and N_3 independently sparsify their local models; (2) N_1 masks the common indices of its model with those of neighbors that are 2 hops away (*i.e.*, N_2 and N_3) and that share a common neighbor (N_r); (3) Indices that were kept unmasked are discarded; (4) N_1 sends the resulting masked model to N_r .

that would be achieved in D-PSGD on the same graph.

The protocol contributes further by integrating sparsification. Sparsification occurs independently among nodes, and there are no mechanisms to ensure that two nodes creating a mask will choose the same set of indices. Consequently, any indices that lie in the symmetric difference of the two nodes' selected indices will lack their corresponding mask, preventing the mask from being canceled out. To address this, the protocol applies a pairwise mask solely to the subset of indices that both parties have selected during sparsification, namely, the intersection of their selected indices. It is important to note that, unlike previously, the number of masks applied to each index of the same node may vary. Additionally, some indices might be selected only by one node and remain unmasked, as they do not form part of any intersection. The protocol therefore counts the number of masks applied to each index, discarding any indices that have no masks applied before sending the masked model. As a result, every transmitted index is masked, and its corresponding opposite mask is included among the other masked models received by the neighboring node. The act of dropping some extra parameters may impact convergence, which we analyse/evaluate in Section 4.6.2.

The protocol is performed in two distinct communication steps. In the first step, denoted as *prestep*, each node coordinates with the neighbors of its neighbors. During this coordination, nodes exchange partial seeds for the pairwise masks and share the set of indices selected in their sparsification process. A node then computes the intersection of its own indices with those received and applies a pairwise mask to this intersection. This pairwise mask is derived by subtracting the sender's generated mask (from their partial seed) from the mask generated by the recipient's own partial seed. Notably, each node produces a distinct partial seed for every other node it interacts with during this phase in each round. In the subsequent step, for each neighbor, a node starts with the unmasked model and applies all pairwise masks agreed

upon with the neighbor's neighbors. It then removes any unmasked indices before transmitting the masked sparse model. Finally, upon receiving these masked models, the recipient node averages them with its model, resulting in a new model ready for training in the next round.

3.4 Theoretical analysis

3.4.1 Privacy guarantees

A parameter is considered private if its exact value cannot be inferred by any other node in the network. A node is considered private if all its parameters are private.

Theorem 1. *CESAR ensures that no honest-but-curious adversary can infer the exact value of any parameter received by its neighbors.*

Proof. Without the loss of generality, let us fix a node $N \in \mathcal{N}$ and consider an arbitrary parameter $p \in I$. During the protocol, node N only receives masked models from its neighbors. If N did not receive the parameter p from any neighbor, it trivially does not learn anything about p .

If N received the parameter p from the neighbor N_{a_0} , it means that N_{a_0} must have applied at least one mask to parameter p . Under CESAR, if N_{a_0} has applied at least one mask, there must be a non-empty exhaustive set of the neighbors $\{N_{a_1}, \dots, N_{a_l}\}$ that share pairwise masks with N_{a_0} for p . Hence, each node of the set $\mathcal{A} = \{N_{a_0}, N_{a_1}, \dots, N_{a_l}\}$ ($|\mathcal{A}| \geq 2$) must have intended to share p . Furthermore, by the algorithm, every pair $\{i, j\}$ of nodes in \mathcal{A} must have agreed on a random pairwise mask $M'_{ij} = -M'_{ji}$ for p . For example, if $v_{N_\ell}^{(p)}$ is a parameter value p at N_ℓ before the protocol and $w_{N_\ell}^{(p)}$ is the value received by N from $N_\ell \in \mathcal{A}$ for parameter p , we know that

$$w_{N_\ell}^{(p)} = v_{N_\ell}^{(p)} + \sum_{N_o \in \mathcal{A} \setminus \{N_\ell\}} M'_{N_\ell N_o}.$$

Because masks are chosen independently from each other, and their values are private to the pair that generated them,

the only way for node N to infer $v_{N_\ell}^{(p)}$ from $w_{N_\ell}^{(p)}$ is to cancel all masks in $w_{N_\ell}^{(p)}$. In order to do this N must add to $w_{N_\ell}^{(p)}$ all values for p received from other nodes that share a pairwise mask with N_ℓ in equal proportion. Therefore, the most node N can infer from the information available to it is the sum of values

$$\sum_{N_\ell \in \mathcal{A}} w_{N_\ell}^{(p)} = \sum_{N_\ell \in \mathcal{A}} v_{N_\ell}^{(p)}.$$

From just the sum no specific contributions can be inferred. \square

3.4.2 Collusion

Environments that involve colluding nodes pose significant challenges. Nevertheless, CESAR can be made resilient against such collusion through simple modifications to Algorithm 1. We suggest that an effective method to counter collusion is to adjust the minimum number of masks applied to an index before its transmission. This change involves implementing a configurable parameter specified by the user of the system, denoted as s , at Line 8 in the algorithm. The modification is represented as $I'_{ik} \leftarrow p \in I : C[p] \geq s$ (i.e. the parameter at position p has to have at least s masks applied in order to be sent, otherwise it is discarded). We call this parameter s as the *masking requirement*. This modification, however, raises concerns about the potential for some masks to be discarded while their corresponding opposite masks are not. Lemma 3 demonstrates that all neighbors of a node, which have selected the parameter at a predetermined position for transmission to the given node, have an identical number of masks applied to the parameter. Moreover, according to the algorithm, every pair of these neighbors agreed on a pairwise mask. Consequently, provided that Assumption 2 is satisfied, it is guaranteed that all such neighbors will either transmit the parameter, thereby cancelling out the masks through aggregation, or conversely, all will discard the parameter and none will transmit it. In other words, we can ensure that all masks cancel out, provided the masking requirement is uniformly applied across the network. In the subsequent analysis, we adhere to the following assumption.

Assumption 2. *All non-colluding nodes must have the same masking requirement when sending their masked models to a fixed neighbor in CESAR.*

Let us consider an environment where the graph has n_t trusted nodes who honestly comply with the protocol and k colluding adversarial nodes who share all the information they have with each other and aim to violate the privacy of the trusted nodes. Let \mathcal{N}_T and \mathcal{N}_A , respectively, denote the sets of the trusted and the colluding adversarial nodes in the graph such that $\mathcal{N} = \mathcal{N}_T \cup \mathcal{N}_A$ and $\mathcal{N}_T \cap \mathcal{N}_A = \emptyset$. In this setting, investigation of the privacy guarantees stays relevant only for the trusted nodes.

Lemma 3. *For a fixed index p the number of masks every node sending their masked models to the same neighbor N_j is either 0 or if not zero the exact same value among all such nodes.*

Proof. The set of indices selected by node $N \in \mathcal{N}$ in sparsification is denoted as $I_N \subseteq I$. We look at the index p and node N_j that receives the masked models. Furthermore we define a set of neighbors of N_j who have selected p in sparsification as $Sel(N_j, p) = \{N \in \text{View}(N_j) : p \in I_N\}$.

For every neighbor $N_i \in \text{View}(N_j)$ there are two cases to consider for index p :

Case 1. $p \notin I_{N_i}$: If N_i does not select p for sharing, by the algorithm there trivially will not be any masks agreed between N_i and another neighbor of N_j , making the number of mask in this case 0.

Case 2. $p \in I_{N_i}$: If N_i selects p for sharing the total number of masks N_i will agree upon with other neighbors of N_j on p is $\text{MaskCount}(N_i, N_j, p) = |\{N \in \text{View}(N_j) \setminus \{N_i\} : p \in I_{N_i \cap N}\}|$. Considering the precondition of the case, expression $p \in I_{N_i \cap N}$ can be transformed into $p \in I_N$ making $\text{MaskCount}(N_i, N_j, p) = |\{N \in \text{View}(N_j) \setminus \{N_i\} : p \in I_N\}|$. Because $p \in I_{N_i}$ then $N_i \in Sel(N_j, p)$, so the previous expression can also be written as $\text{MaskCount}(N_i, N_j, p) = |Sel(N_j, p) \setminus \{N_i\}| = |Sel(N_j, p)| - 1$. Repeating the same for all neighbors of N_j we obtain the exact same value, hence proving the statement of the lemma. \square

Lemma 4. *If the masking requirement of the nodes is k , without worsening the privacy of the trusted nodes, any graph under CESAR, where $|\mathcal{N}_A| \leq k$, can be transformed into a graph where:*

- i. $|\mathcal{N}_A| = k$
- ii. All trusted nodes have a degree of at least 1
- iii. the nodes in \mathcal{N}_A form a clique
- iv. $\{N_i, N_j\} \notin E$ for any $N_i, N_j \in \mathcal{N}_T$

Proof. i. If there are $s < k$ adversarial nodes in the graph, adding an adversarial node with degree 0 will not change the number of masks that the trusted nodes applied to their model parameters.

ii. If there is a trusted node with degree 0, it does not contribute to the working of the protocol or the number of masks that the other trusted nodes decide to apply. Therefore, we may remove them from the graph without compromising the privacy of any of the nodes.

iii. If there is any $N_0 \in \mathcal{N}_A$ without having an adversary as its neighbor, for every $N \in \mathcal{N}_A$, adding $\{N_0, N\}$ to E increments the number of masks added to the parameters of any trusted node connected to N_0 or N by one (which will possibly be shared between N and N'). However, more importantly,

this does not reduce any masks already applied to the parameters of the trusted nodes, implying their privacy remains at least as it was when $\{N_0, N\}$ was not in E .

iv. Let $\{N_i, N_j\} \in E$ for some $N_i, N_j \in \mathcal{N}_T$. Deleting this edge between N_i and N_j will not affect the masks that any trusted node applies to the parameters that they share with the adversarial nodes. We note, however, that deleting the edge between N_i and N_j will reduce the number of masks applied to the parameters that any other trusted node N_ℓ shares with N_i or N_j . But, as N_i or N_j are not involved in any collusion (i.e., have no information about the masks used by any other node), as long as the parameters they receive from N_ℓ have at least one mask applied to them, the privacy of N_ℓ will be upheld. \square

Theorem 5. *If k is the masking requirement of every trusted node in the network, the true values of their model parameters will remain obfuscated from every node in the network when there are k colluding adversarial nodes.*

Proof. By Lemma 4, it is sufficient to consider the case where the trusted nodes have edges only with the adversarial nodes. Setting the number of adversarial nodes as k , as they collude in nature, we assume that they form a k clique in the network. Letting n_t be the number of trusted nodes present in the network, we proceed to show the result by inducting over n_t .

When $n_t = 1$, denoting N to be the only trusted node, as it is connected to an adversarial node A , $|\text{Comm}(A, N)| = k - 1$. Therefore, N can have at most $k - 1$ masks applied to any of its parameters (which are decided by the protocol communicating with the members of $\text{Comm}(A, N)$). As the masking requirement is set to k , N will never end up sharing updates from any of its parameters with A , implying that its true value will never be revealed.

Let the result hold for some $n_t = \lambda - 1 \geq 2$ and a new trusted node in the network. Let the trusted nodes be N_1, \dots, N_λ . Due to Lemma 4, we may ignore any edge between the trusted nodes and only consider the case where they have adversarial neighbors. Let N_i have an edge with adversarial node A_i for every $i \in \{1, \dots, \lambda\}$.

Case 1. $A_\lambda \neq A_i$ for every $i \in \{1, \dots, \lambda - 1\}$: This essentially implies that N_λ can have at most $k - 1$ masks applied its values at any index and, therefore, will not share its model updates with the adversarial nodes and it will remain private.

Case 2. $A_\lambda = A_i$ for some $i \in \{1, \dots, \lambda - 1\}$: If $|\text{Comm}(A_\lambda, N_\lambda)| < k - 1$, the maximum number of masks that N_λ can apply to the value of its model update at any parameter will be less than its masking requirement of k and, hence, will not share its model updates with the adversarial nodes and it will remain private. Otherwise, N_λ and N_i communicate and privately agree to mask their corresponding model updates at the indices in $I_{\lambda \cap i}$ with M_{λ_j} and $M_{j\lambda} (= -M_{\lambda_j})$, respectively.

Thus, $\{v_\lambda^{(p)} : p \in I_{\lambda \cap i}\}$ will have at least one secure mask M_λ applied to it for every $p \in I_{\lambda \cap i}$ which will not be available to the colluding adversarial nodes. Thus, the true values $\{v_\lambda^{(p)}\}$ will remain hidden from A_λ (and, correspondingly, from every other adversarial node) due to the privately chosen mask between N_λ and N_i . \square

Recalling that CESAR discards unmasked indices therefore reducing the percentage of model parameters intended for sharing in sparsification, understanding how this percentage varies based on system parameters, masking requirements, and training configuration is vital to evaluate the practical application of CESAR.

Given the difficulty of exhaustively modeling every sparsification approach, our focus is on a simplified yet realistic scenario. Here, each index is equally likely to be selected for sparsification, and the selection is mutually independent between nodes. While this assumption does not hold for many sparsification methods, it perfectly characterizes random subsampling. We assume that every node chooses α fraction of their indices for sparsification. Since all nodes select the same proportion of parameters and the overall model sizes are identical, the probability $\pi_i^{(p)}$ for any node i to select a given index p is α . Hence, we enable ourselves to derive the expected number of model parameters shared by each node in the network under CESAR capturing an environment when we have k colluding nodes.

Theorem 6. *Under CESAR with random subsampling, if the nodes have a masking requirement of s , setting $\beta(\alpha, \delta, s)$ to be the expected proportion of parameters shared by one node (sender) to another (receiver) in one round, we have:*

$$\beta(\alpha, \delta, s) = \sum_{i=s}^{\delta-1} \binom{\delta-1}{i} \alpha^{i+1} (1-\alpha)^{\delta-1-i}$$

where α is the probability of independently sampling any parameter by any node and $\delta = |\text{View}(\text{Receiver})|$.

Proof. Postponed to Appendix B.1. \square

Corollary 7. *In the absence of any colluding nodes, CESAR with random subsampling ensures that the expected proportion of parameters shared by any node (sender) to another (receiver) in one round is given by:*

$$\beta(\alpha, \delta, 1) = \alpha \left(1 - (1-\alpha)^{\delta-1}\right) \quad (1)$$

where α is the probability of (independently) sampling any parameter by any node and $\delta = |\text{View}(\text{Receiver Node})|$.

Proof. In the absence of collusion, the masking requirement of all the nodes is 1. Thus, putting $s = 1$ in Theorem 6, we

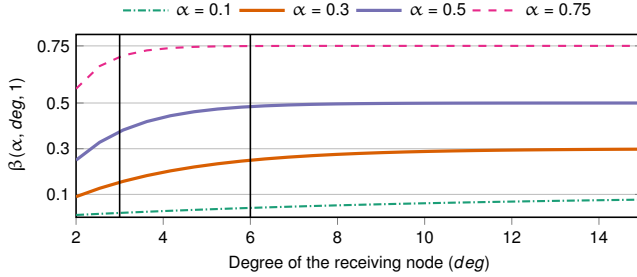


Figure 2: Variation of the fraction of parameters shared in CESAR with the deg denoting the degree of the receiving node and α being the fraction of model parameters selected in sparsification by each node for masking requirement $s = 1$ (*i.e.*, in the absence of any colluding adversarial nodes). Vertical lines and solid curves correspond to scenarios assessed in our empirical evaluation in Section 4.

obtain:

$$\begin{aligned} \beta(\alpha, \delta, 1) &= \alpha \sum_{i=1}^{\delta-1} \binom{\delta-1}{i} \alpha^i (1-\alpha)^{\delta-1-i} \\ &= \alpha \left(1 - (1-\alpha)^{\delta-1} \right) \end{aligned}$$

□

Figure 2 illustrates how β varies with different values of α and degree, based on Equation (1). It is observed that for a sufficiently high degree, the percentage of shared parameters (β) converges towards the percentage of parameters selected in sparsification (α). This convergence occurs more rapidly for higher values of α . Additionally, the relative percentage of discarded parameters appears to be larger for smaller values of α at for the same degree.

3.4.3 Communication overhead

In this analysis, the model size is denoted by d , the fraction of indices selected in sparsification by α , and the maximum degree of any node in the graph by δ_{\max} .

The communication overhead incurred by CESAR occurs primarily in the prestep stage. During this phase, each node dispatches a single message to the neighbors of its neighbors. The number of these message transmissions is bounded by $O(\delta_{\max}^2)$.

Each of these messages comprises a partial seed, which has a size of $O(1)$, and a set of indices selected during sparsification, the size of which is $O(\alpha d)$.

Consequently, the total communication overhead for the prestep in CESAR amounts to $O(\alpha d \delta_{\max}^2)$.

4 Evaluation

In this section, we evaluate the performance of CESAR against a well-regarded baseline, for a variety of graph topologies and different fractions of the model selected in sparsification over three datasets.

4.1 Implementation

The code is implemented in Python 3.6, using *decentralizepy* library [9], which is built on top of PyTorch for machine learning.

4.2 Setup

We conducted our experiments on three machines. Each machine is equipped with 32-core Intel(R) Xeon(R) CPU E5-2630 v3 CPU clocked at 2.40GHz and runs Ubuntu 20.04.4 LTS with the 5.4.0-122-generic kernel. Unless otherwise specified all experiments are carried out on a 48-node network, with each machine simulating 16 nodes. The nodes are organized in a randomly generated k -regular graph in all experiments, *i.e.*, every node has k neighbors where the value of k is specified for each experiment. The size of the network in the experiments stays fixed. We show in Section 3.4.3 that the overhead of the protocol depends only on the degree of nodes rather than the total number of nodes in the network.

Every experiment is run 5 times for different seeds and the results are averaged over them. Masking requirement of CESAR in all experiments is $s = 1$.

4.3 Dataset and hyperparameters

The experiments are conducted on CIFAR-10 [24], CelebA [5] and MovieLens [16]. CIFAR-10 and CelebA are image classification tasks, while MovieLens is a recommendation task.

We partition training dataset among nodes such that no two nodes get the same sample. The whole test set is utilized for performance evaluation at every test step.

Training data is partitioned in one of two ways: IID and non-IID. IID distribution is applied only on CIFAR-10 and CelebA by shuffling the datasets and splitting them into chunks of equal size that are given to each node. The same approach is applied to MovieLens, however it is non-IID by the nature of data. In the case of non-IID, we perform it only on CIFAR-10: the dataset is sorted by the label and split into $2n$ equally sized chunks, where n is the total number of nodes, and each node is given 2 chunks. This limits the total number of classes a node can receive in non-IID partitioning to 4.

The training is performed using SGD optimizer without momentum. The values of hyperparameters are tuned by running a grid search on D-PSGD with full-sharing. Every communication round marks one full execution of CESAR. Test metrics are evaluated at the end of each epoch. The values of

hyperparameters together with the size of data and models used for training are shown in Table 1. They stay the same for all experiments performed on a given dataset.

4.4 Metrics

The performance of CESAR is evaluated using several key metrics. The utility of trained models is measured using test loss and top-1 accuracy on the test set, except for the MovieLens dataset, on which we measure only test loss. Besides utility, we also measure the total amount of data transferred between nodes during training process. This data is partitioned in 3 classes depending on what data is transferred:

- CESAR-specific prestep overhead, which we call *protocol* overhead.
- Masked *model parameters*.
- Additional *metadata* associated with the masked model parameters (e.g., indices).

We compute and record these metrics at the conclusion of each training epoch. For a comprehensive view, each metric is averaged across all nodes and runs, ensuring a robust evaluation of the performance of CESAR.

4.5 Baselines

CESAR is compared against D-PSGD with Metropolis-Hastings weights [46] over random subsampling and TOPK sparsification for different fractions of selected indices. We limit the usage of TOPK on IID data as previous work has shown that it performs poorly in non-IID settings [10].

In all experiments, we use mathematical modelling from Corollary 7 to ensure that the fraction of parameters shared with neighbors in CESAR roughly matches 30 and 50% mark. The actual values we use are shown in Table 2. Furthermore, to ensure that both algorithms share the exact same fraction of parameters we first run CESAR and measure mean fraction of shared weights across all nodes and runs and use the obtained value as the fraction of parameters shared in D-PSGD with the same settings.

Because CESAR works on the basis of obfuscating parameters using masks, we cannot compress the masked parameters. To keep the evaluation consistent, the same is done for D-PSGD. On the other hand, Elias gamma compression [11] is used for compressing indices in both algorithms.

4.6 Performance

In this section, we evaluate CESAR on several metrics against the baseline. First, in Section 4.6.1 we look into the performance of CESAR on several datasets. In Section 4.6.2, we zoom into one of these datasets and do more exhaustive analysis of the performance. Section 4.6.3 looks how CESAR

scales with the size and topology of the network. Finally, Section 4.6.4 provides insights of the security of CESAR in a setting with colluding adversaries.

4.6.1 Evaluation Across Multiple Datasets

In this section, we examine the performance and data usage of CESAR in comparison to D-PSGD across CIFAR-10, CelebA, and MovieLens datasets, with 30% of parameters shared in a 6-regular graph and using the same set of hyperparameters.

Figure 3 presents the results of both algorithms using random subsampling, as well as TOPK. All datasets included in Figure 3b follow IID distribution, and hence the figure excludes MovieLens. In Figure 3a, CIFAR-10 and MovieLens follow non-IID, while CelebA follows IID distribution.

Upon visual inspection, it is evident that CESAR retains performance levels that match D-PSGD while transferring up to 35% more data on TOPK, and significantly less on random subsampling. This indicates that in particular settings, CESAR can be applied in place of D-PSGD without needing to alter hyperparameters.

We also observe that additional data is distributed differently between random subsampling and TOPK. The additional data of protocol (prestep) is negligible in random subsampling, while metadata used to transfer information about model indices increases. In contrast, metadata in TOPK does not change, while most of the data overhead comes from protocol (prestep).

On the implementation level, random subsampling does not need to exchange indices in the prestep, comparably when sending models in D-PSGD. Instead, it can send only a seed used for generating a mask for selecting indices to send to their second-degree neighbors. This results in a negligible overhead since each message is of constant small size. However, when performing an intersection of these masks, the final result must be represented as a set of indices, hence increasing the metadata required for transferring masked model. This increase is dependent on the size of their immediate, rather than second degree neighborhood.

On the other hand, indices selected by TOPK and other non-trivial approaches must be transmitted as full sets, thereby incurring a higher communication overhead for each message sent in the prestep. This set has to be sent to each second degree neighbor, and their number scales with the square of the node degree in the network.

4.6.2 In-Depth Analysis on CIFAR-10

In this section we take a deeper look in the performance of CESAR over various settings on the CIFAR-10 dataset. For IID data, we use TOPK sparsification, and for non-IID, random subsampling. Measurements are taken for 3 and 6-regular graphs at 30% and 50% of parameters intended for

Hyperparameter	Dataset		
	CIFAR-10	CelebA	MovieLens
Learning rate	0.01	0.001	0.05
Batch size	8	8	64
Communication rounds per epoch	21	10	22
SGD steps per communication rounds	6	10	1
Dataset property			
Number of training samples	50000	63741	70000
Dataset type	Image classification	Image classification	Recommendation
Model	4 Conv2D Layers	GN-LeNet [18]	Matrix Factorization [23]
Number of model parameters	89834	30242	206680

Table 1: Training hyperparameters, dataset properties and models trained on them

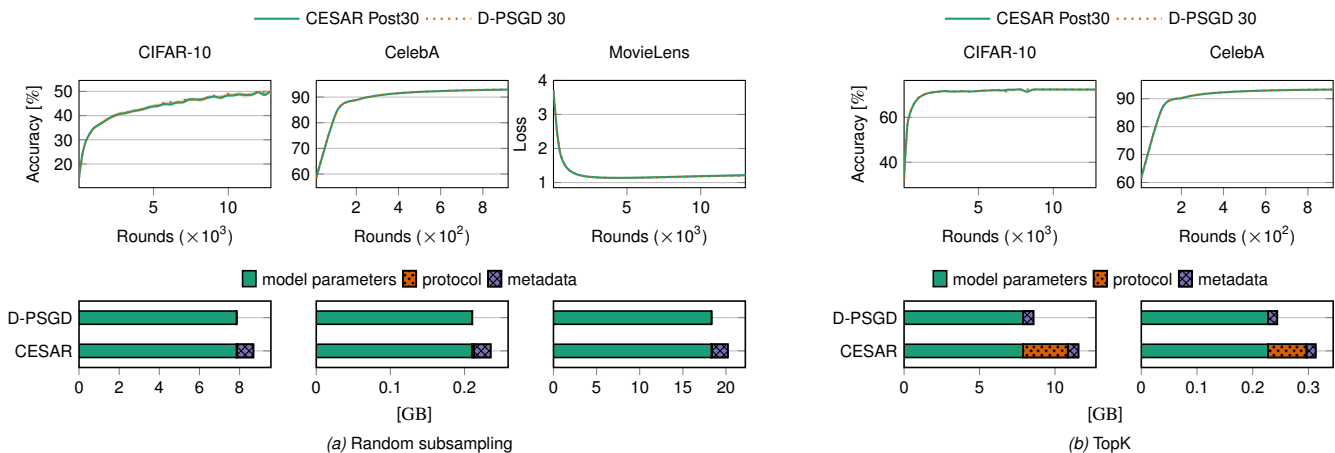


Figure 3: Comparison of performance and communication cost of CESAR against D-PSGD with matching configuration over multiple datasets. CESAR is overlapping D-PSGD in the performance plots

β	α [Degree=3]	α [Degree=6]
30%	43.83%	34.22%
50%	59.70%	51.39%

Table 2: Fraction of parameters required to be selected in sparsification (α) based on the degree of the receiving node and the fraction of parameters intended to be sent to it (β) according to Equation (1)

sharing.

The results are shown in Figure 4 and Table 3. They provide several takeaways. Firstly, the proportion of shared weights using random subsampling is practically the same as our theoretical model predicts. In contrast, TOPK differs. Yet, it is relatively close to the expected values.

The accuracy of CESAR is comparable to that of D-PSGD. When evaluating on non-IID distribution using random sub-

sampling, we observe a decrease in accuracy: a reduction of up to 0.46% on 3-regular graphs, and 0.18% on 6-regular graphs. We suspect this is due to loss of precision in numerical conversion. In order to mask the parameters, we first convert their values from real numbers to integers, retaining only the first six decimal places to fit them into a data type of equivalent size. This process results in slight information loss, which impacts accuracy.

Conversely, CESAR outperforms D-PSGD on IID distribution using the TOPK: showing an improvement of up to 0.3% on 3-regular graphs, and 0.03% on 6-regular graphs. This demonstrates that, under certain conditions, the unique properties of CESAR can enhance learning performance without increasing the fraction of shared parameters. A notable feature of CESAR that may explain this behavior is that every parameter is received from at least two neighbors, which may hypothetically improve generalization of the trained model.

Finally, CESAR induces some data overhead in comparison

to D-PSGD, ranging between 12% and 35% for TOPK, and between 7% and 11% for random subsampling. Furthermore, the behavior of this overhead varies with the degree of the graph. In random subsampling, it remains relatively constant and does not increase with the degree. In contrast, with TOPK we observe a significant increase as we move from degree 3 to 6. Section 4.6.3 looks deeper into this behavior.

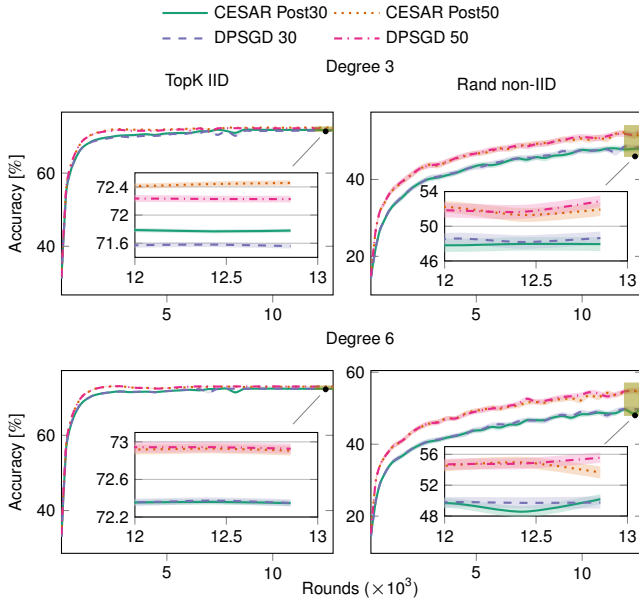


Figure 4: The accuracy comparison of CESAR against D-PSGD over various configurations, data distributions and network degrees

4.6.3 Scalability: Effects of Network Size and Topology

In this section, we examine how the communication overhead of CESAR scales in practice. As observed in Section 4.6.1 and Section 4.6.2, the overhead with random subsampling remains constant regardless of the network topology. In contrast, it increases when TOPK is applied.

Section 3.4.3 derives that the communication overhead of the prestep in CESAR is $(\alpha d \delta_{\max}^2)$, as a node sends their indices to each second degree neighbor, and their number typically scales with the square of the degree in the network. To verify this, we ran CESAR with TOPK on a 96-node k -regular network with k values of 3, 6, 9, and 12. In each run, 40% of parameters were selected for sparsification, and we recorded only the overhead caused by the protocol (prestep).

The results for the given degrees are shown in Figure 5. They indicate that the overhead scales linearly, contrary to the quadratic scaling we expected. However, Table 4 reveals that the overhead of the prestep actually scales with the size of the second degree neighborhood. Because the network size

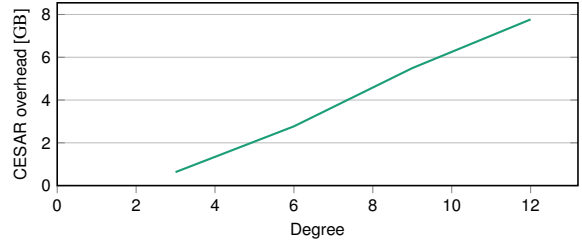


Figure 5: Amount of data transferred per node in CESAR prestep during training for different graph degrees

is limited, it is common for two nodes to share a neighbor, hence reducing the size of the second degree neighborhood compared to a theoretical model where the network size is infinite and nodes sharing a neighbor are uncommon. This also implies that the total overhead of the prestep is limited by the size of the network to $(\alpha d |\mathcal{N}|)$. This underscores the importance of the ability of CESAR to reuse masks that two nodes agreed upon when sharing their masked models with multiple common neighbors.

4.6.4 Configuring for Minimized Collusion Risks

Section 3.4.2 shows formal privacy guarantees in systems where the number of adversaries is known. However, this is often not the case, and the number of adversaries has to be estimated. Therefore, we look at how the privacy risk changes as we increase the masking requirement (s) in CESAR for a 25-regular graph with 100 nodes in settings with different number of adversaries.

This is performed by running a Monte Carlo simulation 250 000 times for each masking requirement. Each simulation involves generating a random 25-regular graph and assigning each node to be either adversarial or honest. All adversarial nodes are assumed to collude with each other. Over the simulation, we measure the probability that any honest node in the network is at risk of adversaries. A node is considered to be at risk if any of their parameters can be inferred by the adversaries. This can only happen when the node is connected to an adversary who has at least s adversarial neighbors.

The simulation results are shown in Figure 6. The results reveal that even for masking requirement lower than the total number of adversaries, yet sufficiently high, the risk can be practically nonexistent to any node in the network. For instance, for the setting with 15 adversaries we do not come across any graphs under risk for masking requirement ≥ 13 in any of our simulations. Furthermore, with masking requirement 9 the risk is 1.45% in this setting.

5 Related work

Privacy attacks. We are seeing continuous work on privacy attacks against ML models in distributed machine learning.

Data distribution	Sparsification	Degree	Proportion of shared weights [%]	Algorithm	Maximum achieved accuracy [%]	Total data transferred [GB]
IID	TOPK	3	31.02	CESAR	71.88	5.22
				D-PSGD	71.58	4.41
		6	50.48	CESAR	72.50	7.90
				D-PSGD	72.29	7.03
non-IID	random subsampling	3	30.13	CESAR	72.42	11.56
				D-PSGD	72.40	8.58
		6	49.67	CESAR	73.12	17.28
				D-PSGD	73.09	13.83

Table 3: The performance of CESAR against D-PSGD over regular graphs of various degrees and fractions of model shared

Degree	CESAR overhead [GB]	Average 2^{nd} degree neighborhood size	CESAR overhead per 2^{nd} degree neighbor [GB]
3	0.63	5.93	0.1064
6	2.77	26.87	0.1031
9	5.49	53.48	0.1027
12	7.77	75.16	0.1034

Table 4: Amount of data transferred per node in CESAR prestep during training for different graph degrees and their relation to the size of second degree neighborhood

Gradient inversion [14, 51], membership inference [40], and attribute inference attacks [50] are commonly employed to extract information about the training set from the exchanged models. Both gradient inversion and membership inference have been also shown to be effective against D-PSGD [32]. While sparsification has been suggested as a defense against privacy attacks [38, 45, 51], Yue *et al.* [49] present a gradient inversion attack on gradients sparsified with TOPK. These attacks, however, are not well understood under the presence of secure aggregation. Furthermore, the masks in CESAR can be considered as perturbations of model parameters in noise-based defenses against privacy attacks in ML [8, 44, 48]. Since privacy attacks to averaged models would succeed in CESAR

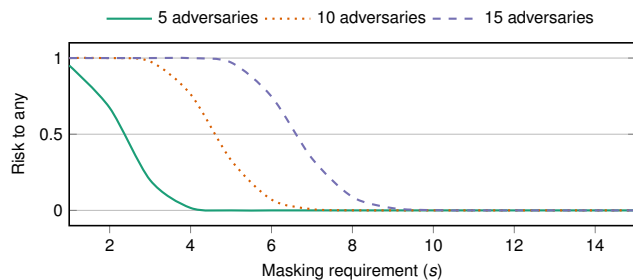


Figure 6: Estimated attack risk to any honest node in randomly generated 100 node graph with 25-regular topology

in the same way they would in any other secure aggregation scheme, we consider them orthogonal to this work.

Secure aggregation. Secure aggregation works on the principle of obfuscating local models and making only the aggregated model public, hence making attacks harder to perform. It has been a prominent approach for keeping models secure in FL setting. The majority of work in this field is based on ideas proposed by [4]: pairwise additive masking, node-specific masks and the use of Shamir [37] secret sharing for recovery when nodes fail. In comparison, work on secure aggregation in DL setting is limited [15], and often involves additional servers [17]. Additionally, integrating data reduction techniques within secure aggregation presents significant

challenges, particularly in environments where data usage is limited. In comparison to existing secure aggregations in DL, our solution is the first that includes sparsification in its core structure while avoiding use of additional servers.

Secure aggregation with sparsification. Reduction of model size is a prominent research topic, ranging from compression [7, 33], sparsification [27, 39, 41] and quantization [2, 36], as well as other techniques [10, 22]. However, there is limited research done in incorporating these approaches into secure aggregation. Most of this research has been limited to FL. SparseSecAgg [12] pioneers the integration of sparsification with secure aggregation. Their method integrates a sparsification mechanism directly into the aggregation protocol, albeit with limitations in compatibility with other sparsification techniques. Lu *et al.* [29] advance this field further, incorporating TOPK sparsification as a part of their protocol. This work also raises the concern of information leakage caused by sharing the set of indices selected in sparsification with other nodes, and proposes adding additional randomly selected indices to reduce the risk. Their approach shows resemblance to ours, even though in FL setting, as it focuses on masking union of indices selected by different nodes, rather than their intersection like we do. Nevertheless, considering both are designed for FL they rely on the presence of a central node and hence they cannot be trivially adapted to DL setting.

6 Discussion

Limited selection of sparsification approaches. While the paper focuses on random subsampling and TOPK for sparsification, other approaches can also be used in their place interchangeably. However, certain sparsifications rely on storing additional information and carrying them from one round to another, often for the purpose of error compensation. They are often designed with an assumption that their result is sent without changes to all neighbours in the same form, but CESAR takes the result of sparsification and sends a different subsets of it to each neighbor. Therefore, branching the state for each neighbor without an obvious way to merge them into one state usable for the next round of sparsification. Hence, CESAR does not support sparsifications that rely on carrying information of their choices from previous rounds in order to perform parameter selection in the current round.

Disconnecting nodes. While CESAR shows good performance, it does not support nodes dropping out. In FL literature Shamir’s secret sharing [37] is often used to remove secrets of disconnected nodes. However, in comparison, in DL the size of individual aggregation is determined by the degree of a node, which is often relatively small. Therefore, we assume that dropping out of nodes in this setting may be relatively in-

frequent, but also too expensive to recover from in same way done in FL. We hypothesize that starting the protocol from the beginning may be a cheaper way to recover when dropouts occur. Furthermore, as pairwise masks remain private there would be no need to rerun the prestep of the protocol, and instead use the data received in the initial attempt. However, these claims are out of the scope of this paper and they need extensive testing.

7 Conclusion

This paper presented CESAR, a novel secure aggregation protocol tailored for DL training. CESAR addresses the unique challenges posed by integrating secure aggregation with various sparsification techniques, a crucial concern in decentralized learning for preserving privacy and enhancing communication efficiency. Our protocol effectively balances the trade-offs between privacy preservation, communication overhead, and model accuracy.

The experimental results demonstrate that CESAR, when combined with random subsampling, matches the performance of D-PSGD while only adding a modest increase in data overhead. Additionally, CESAR outperforms TOPK sparsification methods in accuracy, underscoring its effectiveness in maintaining model quality. These achievements are significant in the context of decentralized learning, where efficient communication and robust privacy are crucial.

Furthermore, the adaptability of CESAR to different forms of sparsification and its robustness against honest-but-curious adversaries, with potential adaptations for collusion resistance, mark it as a versatile and secure solution for DL scenarios.

Future work could explore further optimization of CESAR for different network topologies and more complex models, as well as its combination with other sparsification techniques. The integration of CESAR in real-world applications promises to significantly contribute to the advancement of secure, efficient, and privacy-preserving decentralized machine learning systems.

References

- [1] Gergely Ács and Claude Castelluccia. I have a dream!(differentially private smart metering). In *International Workshop on Information Hiding*, pages 118–132. Springer, 2011.
- [2] Dan Alistarh, Demjan Grubic, Jerry Z. Li, Ryota Tomioka, and Milan Vojnovic. QSGD: Communication-efficient SGD via gradient quantization and encoding. In *NIPS*, 2017.
- [3] Dan Alistarh, Torsten Hoefler, Mikael Johansson, Sarit Khirirat, Nikola Konstantinov, and Cédric Renggli. The

- convergence of sparsified gradient methods. In *NeurIPS*, 2018.
- [4] Keith Bonawitz, Vladimir Ivanov, Ben Kreuter, Antonio Marcedone, H Brendan McMahan, Sarvar Patel, Daniel Ramage, Aaron Segal, and Karn Seth. Practical secure aggregation for privacy-preserving machine learning. In *proceedings of the 2017 ACM SIGSAC Conference on Computer and Communications Security*, pages 1175–1191, 2017.
- [5] Sebastian Caldas, Sai Meher Karthik Duddu, Peter Wu, Tian Li, Jakub Konečný, H. Brendan McMahan, Virginia Smith, and Ameet Talwalkar. Leaf: A benchmark for federated settings, 2019.
- [6] Mingqing Chen, Rajiv Mathews, Tom Ouyang, and Françoise Beaufays. Federated learning of out-of-vocabulary words.
- [7] Yann Collet. LZ4, 2022.
- [8] Edwige Cyffers, Mathieu Even, Aurélien Bellet, and Laurent Massoulié. Muffliato: Peer-to-peer privacy amplification for decentralized optimization and averaging. In *Advances in Neural Information Processing Systems (NeurIPS '22)*, 2022.
- [9] Akash Dhasade, Anne-Marie Kermarrec, Rafael Pires, Rishi Sharma, and Milos Vujanovic. Decentralized learning made easy with decentralizepy. In *Proceedings of the 3rd Workshop on Machine Learning and Systems*, pages 34–41, 2023.
- [10] Akash Dhasade, Anne-Marie Kermarrec, Rafael Pires, Rishi Sharma, Milos Vujanovic, and Jeffrey Wigger. Get more for less in decentralized learning systems. In *2023 IEEE 43rd International Conference on Distributed Computing Systems (ICDCS '23)*, pages 463–474, 2023.
- [11] Peter Elias. Universal codeword sets and representations of the integers. *IEEE transactions on information theory*, 21(2):194–203, 1975.
- [12] Irem Ergun, Hasin Us Sami, and Basak Guler. Sparsified secure aggregation for privacy-preserving federated learning. *arXiv preprint arXiv:2112.12872*, 2021.
- [13] European Commission. Fundamental texts on european private law, 2016.
- [14] Jonas Geiping, Hartmut Bauermeister, Hannah Dröge, and Michael Moeller. Inverting gradients - how easy is it to break privacy in federated learning? In *Advances in Neural Information Processing Systems (NeurIPS '20)*, volume 33, pages 16937–16947, 2020.
- [15] Nirupam Gupta, Jonathan Katz, and Nikhil Chopra. Privacy in distributed average consensus**this work was supported by the naval air warfare center aircraft division - pax river, md under contract n00421132m022. *IFAC-PapersOnLine*, 50(1):9515–9520, 2017. 20th IFAC World Congress.
- [16] F. Maxwell Harper and Joseph A. Konstan. The movielens datasets: History and context. *ACM Trans. Interact. Intell. Syst.*, 5(4), dec 2015.
- [17] Lie He, An Bian, and Martin Jaggi. Cola: Decentralized linear learning. *Advances in Neural Information Processing Systems*, 31, 2018.
- [18] Kevin Hsieh, Amar Phanishayee, Onur Mutlu, and Phillip B. Gibbons. The non-IID data quagmire of decentralized machine learning. In *ICML*, 2020.
- [19] Li Huang, Yifeng Yin, Zeng Fu, Shifa Zhang, Hao Deng, and Dianbo Liu. LoAdaBoost: loss-based AdaBoost federated machine learning with reduced computational complexity on IID and non-IID intensive care data.
- [20] Abhinav Jain, Hima Patel, Lokesh Nagalapatti, Nitin Gupta, Sameep Mehta, Shanmukha Guttula, Shashank Mujumdar, Shazia Afzal, Ruhi Sharma Mittal, and Vitotha Munigala. Overview and importance of data quality for machine learning tasks. In *Proceedings of the 26th ACM SIGKDD International Conference on Knowledge Discovery & Data Mining*, pages 3561–3562. ACM.
- [21] Daniel Jarrett, Eleanor Stride, Katherine Vallis, and Mark J. Gooding. Applications and limitations of machine learning in radiation oncology. 92(1100):20190001.
- [22] Anastasia Koloskova, Sebastian Stich, and Martin Jaggi. Decentralized stochastic optimization and gossip algorithms with compressed communication. In *ICML*, 2019.
- [23] Yehuda Koren, Robert Bell, and Chris Volinsky. Matrix factorization techniques for recommender systems. *Computer*, 42(8):30–37, aug 2009.
- [24] Alex Krizhevsky, Vinod Nair, and Geoffrey Hinton. The cifar-10 dataset. 55(5), 2014.
- [25] Anusha Lalitha, Tara Javidi, Shubhanshu Shekhar, and Farinaz Koushanfar. Fully decentralized federated learning.
- [26] Xiangru Lian, Ce Zhang, Huan Zhang, Cho-Jui Hsieh, Wei Zhang, and Ji Liu. Can decentralized algorithms outperform centralized algorithms? a case study for decentralized parallel stochastic gradient descent. In *NIPS*, 2017.

- [27] Yujun Lin, Song Han, Huizi Mao, Yu Wang, and Bill Dally. Deep gradient compression: Reducing the communication bandwidth for distributed training. In *ICLR*, 2018.
- [28] Dianbo Liu, Dmitriy Dligach, and Timothy Miller. Two-stage federated phenotyping and patient representation learning. In *Proceedings of the 18th BioNLP Workshop and Shared Task*, pages 283–291. Association for Computational Linguistics.
- [29] Shiwei Lu, Ruihu Li, Wenbin Liu, Chaofeng Guan, and Xiaopeng Yang. Top-k sparsification with secure aggregation for privacy-preserving federated learning. *Computers & Security*, 124:102993, 2023.
- [30] H Brendan McMahan, Eider Moore, Daniel Ramage, and Seth Hampson. Communication-efficient learning of deep networks from decentralized data.
- [31] Róbert Ormándi, István Hegedűs, and Márk Jelasity. Gossip learning with linear models on fully distributed data. *Concurrency and Computation: Practice and Experience*, 25(4), 2013.
- [32] Dario Pasquini, Mathilde Raynal, and Carmela Troncoso. On the (in) security of peer-to-peer decentralized machine learning. In *2023 IEEE Symposium on Security and Privacy (SP)*, pages 418–436, 2023.
- [33] Igor Pavlov. LZMA SDK, 2022.
- [34] Swaroop Ramaswamy, Rajiv Mathews, Kanishka Rao, and Françoise Beaufays. Federated learning for emoji prediction in a mobile keyboard.
- [35] Christopher A. Ramezan, Timothy A. Warner, Aaron E. Maxwell, and Bradley S. Price. Effects of training set size on supervised machine-learning land-cover classification of large-area high-resolution remotely sensed data. 13(3):368.
- [36] Frank Seide, Hao Fu, Jasha Droppo, Gang Li, and Dong Yu. 1-bit stochastic gradient descent and application to data-parallel distributed training of speech DNNs. In *Interspeech 2014*, September 2014.
- [37] Adi Shamir. How to share a secret. *Communications of the ACM*, 22(11):612–613, 1979.
- [38] Reza Shokri and Vitaly Shmatikov. Privacy-preserving deep learning. In *Proceedings of the 22nd ACM SIGSAC conference on computer and communications security*, pages 1310–1321, 2015.
- [39] Reza Shokri and Vitaly Shmatikov. Privacy-preserving deep learning. In *2015 53rd Annual Allerton Conference on Communication, Control, and Computing (Allerton)*, pages 909–910, 2015.
- [40] Reza Shokri, Marco Stronati, Congzheng Song, and Vitaly Shmatikov. Membership inference attacks against machine learning models. In *2017 IEEE Symposium on Security and Privacy, SP 2017, San Jose, CA, USA, May 22-26, 2017*, pages 3–18, 2017.
- [41] Nikko Strom. Scalable distributed DNN training using commodity GPU cloud computing. In *16th Annual Conference of the International Speech Communication Association*, 2015.
- [42] Zhenheng Tang, Shaohuai Shi, and Xiaowen Chu. Communication-efficient decentralized learning with sparsification and adaptive peer selection. In *2020 IEEE 40th International Conference on Distributed Computing Systems (ICDCS)*, 2020.
- [43] United States Congress. Health insurance portability and accountability act of 1996.
- [44] Kang Wei, Jun Li, Ming Ding, Chuan Ma, Hang Su, Bo Zhang, and H Vincent Poor. User-level privacy-preserving federated learning: Analysis and performance optimization. *IEEE Transactions on Mobile Computing*, 21(9):3388–3401, 2021.
- [45] Wenqi Wei, Ling Liu, Margaret Loper, Ka-Ho Chow, Mehmet Emre Gursoy, Stacey Truex, and Yanzhao Wu. A framework for evaluating client privacy leakages in federated learning. In *Computer Security—ESORICS 2020: 25th European Symposium on Research in Computer Security, ESORICS 2020, Guildford, UK, September 14–18, 2020, Proceedings, Part I 25*, pages 545–566. Springer, 2020.
- [46] Lin Xiao and Stephen Boyd. Fast linear iterations for distributed averaging. *Systems & Control Letters*, 53(1):65–78, 2004.
- [47] Timothy Yang, Galen Andrew, Hubert Eichner, Haicheng Sun, Wei Li, Nicholas Kong, Daniel Ramage, and Françoise Beaufays. Applied federated learning: Improving google keyboard query suggestions.
- [48] Da Yu, Huishuai Zhang, Wei Chen, and Tie-Yan Liu. Do not let privacy overbill utility: Gradient embedding perturbation for private learning. *arXiv preprint arXiv:2102.12677*, 2021.
- [49] Kai Yue, Richeng Jin, Chau-Wai Wong, Dror Baron, and Huaiyu Dai. Gradient obfuscation gives a false sense of security in federated learning. In *32nd USENIX Security Symposium (USENIX Security 23)*, pages 6381–6398, 2023.
- [50] Benjamin Zi Hao Zhao, Aviral Agrawal, Catisha Coburn, Hassan Jameel Asghar, Raghav Bhaskar, Mohamed Ali Kaafar, Darren Webb, and Peter Dickinson. On the

(in) feasibility of attribute inference attacks on machine learning models. In *2021 IEEE European Symposium on Security and Privacy (EuroS&P)*, pages 232–251. IEEE, 2021.

- [51] Ligeng Zhu, Zhijian Liu, and Song Han. Deep leakage from gradients. *Advances in neural information processing systems (NeurIPS '19)*, 32, 2019.
- [52] Xiangxin Zhu, Carl Vondrick, Charless C. Fowlkes, and Deva Ramanan. Do we need more training data? 119(1):76–92.

A Scalability

In this section, we examine how the communication cost of CESAR scales with an increasing number of nodes in the network. Measurements were conducted for networks comprising 48, 96, 192, and 288 nodes. Each experiment was performed within a 5-regular network using the CIFAR-10 dataset. The dataset was divided into 288 equally-sized segments, corresponding to the maximum node count, with each node receiving one segment. In cases where the number of segments surpassed the number of nodes, the excess segments remained unassigned and were not utilized in the training process.

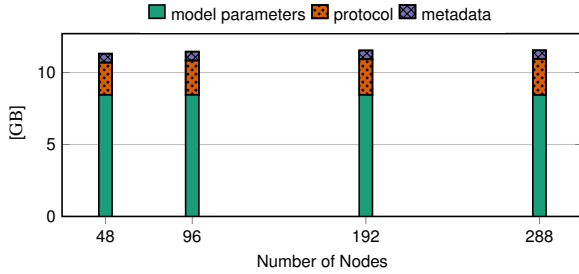


Figure 7: Amount of data transferred per node during training for different number of nodes

Number of nodes	Parameter data [GB]	CESAR overhead [GB]
48	9.07	2.25
96	9.07	2.39
192	9.06	2.48
288	9.05	2.49

Table 5: Amount of data transferred per node during training using CESAR for a fixed setup in networks of different sizes

Figure 7 illustrates that the communication overhead of CESAR remains practically independent of the number of nodes in the network. However, a more detailed examination in Table 5 reveals a marginally higher CESAR overhead for

larger networks. This phenomenon can be attributed to the experimental setup. As discussed in Section 3.4.3, the number of messages sent during the prestep phase of CESAR is proportional to the number of second degree neighbors. With fewer nodes in the network, while maintaining a fixed topology, it is more likely for two neighbors to share a common neighbor. This overlap effectively reduces the average second degree neighborhood size, thereby lowering the overhead in the prestep.

B Postponed Proofs

B.1 Proof of Theorem 6

Proof. Random subsampling ensures that the sparsification selects indices with uniform probability α and we assume that the sparsification carried out by each node is independent.

Without the loss of generality, let us consider the nodes $N, N' \in \mathcal{N}$ where N is the sender and N' is the receiver (i.e., $\{N, N'\} \in E$). With the masking requirement of s , we note that N shares a parameter with N' iff it has been sampled by at least s other neighbors of N' . Therefore, the probability $\hat{\pi}_{N \rightarrow N'}^{(p)}$ of N sharing a parameter $p \in I$ with N' in one round of CESAR is given by:

$$\begin{aligned} \hat{\pi}_{N \rightarrow N'}^{(p)} &= \pi_i^{(p)} \left(1 - \prod_{j \in \text{View}_2(N)} (1 - \pi_j^{(p)}) \right) \\ &= \alpha \sum_{i=s}^{\delta-1} \binom{\delta-1}{i} \alpha^i (1-\alpha)^{\delta-1-i} \\ &= \sum_{i=s}^{\delta-1} \binom{\delta-1}{i} \alpha^{i+1} (1-\alpha)^{\delta-1-i} \end{aligned}$$

Hence, let $X_{N \rightarrow N'}$ be the random variable denoting the number of parameters that N shares with N' in one round with a masking requirement of s , and for every $p \in I$, let $X_{N \rightarrow N'}(p) = \mathbb{I}_{\{N \text{ shares } p \text{ with } N'\}}$ be the random variable denoting whether or not N shares the parameter p with N' . Therefore, noting that $X_{N \rightarrow N'} = \sum_{p \in I} X_{N \rightarrow N'}(p)$, we have:

$$\begin{aligned} \mathbb{E}[X_{N \rightarrow N'}] &= \mathbb{E} \left[\sum_{p \in I} X_{N \rightarrow N'}(p) \right] \\ &= \sum_{p \in I} \mathbb{E}[X_{N \rightarrow N'}(p)] \\ &= \sum_{p \in I} \mathbb{P}[\{N \text{ shares } p \text{ with } N'\}] \\ &= d \hat{\pi}_{N \rightarrow N'}^{(p)} \end{aligned}$$

Thus, the expected fraction of the model parameters that N

shares with N' is given by:

$$\begin{aligned}\beta(\alpha, \delta, s) &= \mathbb{E} \left[\frac{X_{N \rightarrow N'}}{d} \right] \\ &= \frac{\mathbb{E}[X_{N \rightarrow N'}]}{d} \\ &= \hat{\pi}_{N \rightarrow N'}^{(p)} \\ &= \sum_{i=s}^{\delta-1} \binom{\delta-1}{i} \alpha^{i+1} (1-\alpha)^{\delta-1-i}\end{aligned}$$

□